

## Collision-induced spin depolarization of alkali-metal atoms in cold $^3\text{He}$ gas

T. V. Tscherbul,<sup>1,2</sup> P. Zhang,<sup>2</sup> H. R. Sadeghpour,<sup>2</sup> A. Dalgarno,<sup>1,2</sup> N. Brahms,<sup>1,3</sup> Y. S. Au,<sup>1,3</sup> and J. M. Doyle<sup>1,3</sup>

<sup>1</sup>Harvard-MIT Center for Ultracold Atoms, Cambridge, Massachusetts 02138, USA

<sup>2</sup>Institute for Theoretical Atomic, Molecular, and Optical Physics, Harvard-Smithsonian Center for Astrophysics, Cambridge, Massachusetts 02138, USA

<sup>3</sup>Department of Physics, Harvard University, Cambridge, Massachusetts 02138, USA

(Received 3 October 2008; published 31 December 2008)

We present a joint experimental and theoretical study of spin depolarization in collisions of alkali-metal atoms with  $^3\text{He}$  in a magnetic field. A rigorous quantum theory for spin-changing transitions is developed and applied to calculate the spin exchange and spin relaxation rates of Li and K atoms in cryogenic  $^3\text{He}$  gas. Magnetic trapping experiments provide upper bounds to the spin exchange rates for Li- $^3\text{He}$  and K- $^3\text{He}$ , which are in agreement with the present theory. Our calculations demonstrate that the alkali-metal atoms have extremely slow spin depolarization rates, suggesting a number of potential applications in precision spectroscopy and quantum optics.

DOI: 10.1103/PhysRevA.78.060703

PACS number(s): 34.50.-s

Spin-polarized atoms and molecules are key components of research in many areas of physics ranging from atomic magnetometry [1,2] and cryogenic cooling [3,4] to nuclear physics [5] and medical imaging [6]. Collisions of spin-polarized atoms with background gas or other atoms may lead to spin depolarization, causing loss of coherence [7], reduction of the lifetime of trapped atoms [3], and collisional frequency shifts in atomic clocks and magnetometers [1,2]. A particularly important mechanism in which spin polarization is not destroyed but is transferred from one atom to another is known as spin exchange [1,8]. This process underlies the powerful technique of spin exchange optical pumping [8], which is used to polarize the nuclear spins of rare-gas atoms for studies in magnetic resonance imaging [6] and neutron spin structure [5]. Collisions may also lead to spin relaxation which, unlike spin exchange, is always undesirable [1]. A large ratio of the cross sections for spin exchange and spin relaxation is therefore essential for the efficiency of spin exchange optical pumping [8,9].

The potential and versatility of the buffer-gas cooling method [3] in producing cold trapped ensembles of atoms and molecules at temperatures below 1 K have been demonstrated by a number of recent experiments [4]. The cooling starts by introducing hot atoms in a cell filled with cryogenic  $^3\text{He}$  gas. Elastic collisions quickly refrigerate the atoms to subkelvin temperatures, so they can be confined in a magnetic trap [3]. The lifetime of atoms in the trap is limited by spin relaxation due to collisions with the buffer-gas atoms. A large ratio of the cross sections for elastic collisions and spin relaxation is required for efficient cryogenic cooling. Therefore, understanding the mechanisms of collision-induced spin exchange and spin relaxation is essential for the success of both cryogenic cooling and spin exchange optical pumping, even though the two techniques may operate in different temperature regimes.

Previous theoretical work has shown that spin exchange in collisions of alkali-metal atoms ( $M$ ) with  $^3\text{He}$  occurs due to the Fermi contact hyperfine interaction between the electron spin of the alkali-metal atom and the nuclear spin of  $^3\text{He}$  [8,10]. The strength of the hyperfine interaction is propor-

tional to the unpaired spin density at the He nucleus defined as  $\varrho(R) = \langle \psi(\mathbf{r}_e, \sigma; R) | \delta(\mathbf{r}_e) | \psi(\mathbf{r}_e, \sigma; R) \rangle$ , where  $\delta(\mathbf{r}_e)$  is the Dirac delta function,  $\psi(\mathbf{r}_e, \sigma; R)$  is the adiabatic electronic wave function for the ground  $^2\Sigma$  electronic state of  $M\text{-}^3\text{He}$ , and the averaging is performed over the spatial ( $\mathbf{r}_e$ ) and spin ( $\sigma$ ) coordinates of the electrons defined in the frame with the origin at the  $^3\text{He}$  nucleus at a fixed internuclear distance  $R$  [10]. Herman [10] proposed a model linking the spin density of the  $M\text{-}^3\text{He}$  complex to that of the isolated alkali-metal atom

$$\varrho(R) = |\eta\phi_n(R)|^2, \quad (1)$$

where  $\phi_n(R)$  is the wave function of the alkali-metal valence electron and  $\eta$  is an enhancement factor due to the exchange interaction between the valence electron of  $M$  and the He core [10]. The most recent estimates for  $|\eta| = 5.8\text{--}12.6$  are based on the frequency shift measurements for Na, K, and Rb in a gas of  $^3\text{He}$  [11–13]. The accuracy of these estimates is, however, limited by the uncertainties in the  $M\text{-He}$  interaction potentials used to extract  $\eta$  from the measured frequency shifts [11].

Here, we present an experimental and theoretical analysis of spin exchange and spin relaxation in collisions of the alkali-metal atoms with  $^3\text{He}$ . The  $^7\text{Li}$  or  $^{39}\text{K}$  atoms are confined in a magnetic trap, and an upper limit to the spin-changing cross section is determined by monitoring the decay of atoms in the trap. For Li- $^3\text{He}$ , we carry out accurate calculations of the electronic structure and collision dynamics without any adjustable parameters. For heavier alkali-metal atoms, we propose a refined estimate for  $\eta$  based on *ab initio* interaction potentials [14] and recent precision measurements of the frequency shift enhancement factors [13]. Our quantum scattering calculations show that collision-induced  $M\text{-}^3\text{He}$  spin exchange and spin relaxation are strongly suppressed at temperatures below 1 K. This suggests that the alkali-metal atoms in a cryogenic bath of  $^3\text{He}$  may be used in a number of applications in precision spectroscopy, quantum optics, and quantum information processing.

TABLE I. Measured lower limits for the ratio of diffusion to spin depolarization cross sections for Li-<sup>3</sup>He ( $T=240 \pm 20$  mK) and K-<sup>3</sup>He ( $T=320 \pm 20$  mK). The confidence limit for the ratios is 97%. The theoretical ratios are for a magnetic field of 2 T.

Atom	$\tau_0$ (s)	$\tau_{\text{trap}}$ (s)	$\bar{\sigma}_D/\bar{\sigma}_R$ Expt.	$\bar{\sigma}_D/\bar{\sigma}_R$ Theory
Li	$0.027 \pm 0.001$	$5.6 \pm 0.5$	$\geq 5.4 \times 10^5$	$1.2 \times 10^{11}$
K	$0.89 \pm 0.03$	$28.6 \pm 0.7$	$\geq 1.1 \times 10^8$	$3.7 \times 10^{11}$

We measure the ratio of the thermally averaged diffusion cross section  $\bar{\sigma}_D$  to the relaxation cross section  $\bar{\sigma}_R$  by confining a cloud of Li or K within a magnetic trap using the apparatus described in [4]. A large density of <sup>3</sup>He is present within the trap, at the same temperature as the trapped alkali-metal atoms. Atoms can be lost due to evaporation over the trap edge or from any number of inelastic loss processes. A lower limit for  $\bar{\sigma}_D/\bar{\sigma}_R$  is set by assuming that all inelastic loss is due to collisional spin depolarization. With this assumption, the lifetime of atoms in the trap is [4]

$$\tau_{\text{trap}} = \frac{\tau_0}{e^{-0.31\bar{\eta}-0.018\bar{\eta}^2} + g\bar{v}_\mu^2\bar{\sigma}_R\tau_0^2/\bar{\sigma}_D}, \quad (2)$$

where  $\bar{\eta} \equiv \mu_B B_{\text{trap}}/k_B T$  is the ratio of the trap depth to the atom temperature,  $\bar{v}_\mu$  is the average relative collision velocity,  $\tau_0$  is the lifetime of atoms diffusing through the helium gas when the trap is turned off, and  $g$  is a geometric factor, equal to  $0.17 \text{ cm}^{-2}$  in our experiment. The probability for spin depolarization is small, and the trap lifetime is limited by evaporative loss rather than inelastic collisions. The upper limit to  $\bar{\sigma}_R$  is therefore determined by the temperature (or  $\bar{\eta}$ ) and lowest  $M$ -<sup>3</sup>He mean free path at which the atoms can be seen with acceptable signal-to-noise ratio. The minimum temperature and maximum helium density will vary with the alkali-metal atom due to variations in both the  $M$ -<sup>3</sup>He elastic cross section and the amount of energy necessary for ablation. To find the lower limit for  $\bar{\sigma}_D/\bar{\sigma}_R$ , we first measure  $\tau_0$  with the trap turned off. We then energize and reload the trap to measure  $\tau_{\text{trap}}$ . Temperature is measured using a thermometer in thermal contact with <sup>3</sup>He. We solve (2) for  $\bar{\sigma}_D/\bar{\sigma}_R$ . Taking into account our measurement uncertainties, we are able to derive lower limits to the ratios. They are given in Table I. We note that the experimental results are entirely consistent with  $\bar{\sigma}_R=0$ , and the larger ratio of  $\tau_0$  to  $\tau_{\text{trap}}$  for Li is due to the lower trapping temperature used.

The Hamiltonian of the  $M$ -<sup>3</sup>He collision complex in the presence of an external magnetic field  $B$  can be written in atomic units as [8]

$$\hat{H} = -\frac{1}{2\mu R} \frac{\partial^2}{\partial R^2} R + \frac{\hat{\ell}^2}{2\mu R^2} + V(R) + \hat{H}_{\text{sd}}(R) + \hat{H}_M + \hat{H}_{\text{He}}, \quad (3)$$

where  $\mu$  is the reduced mass of the complex,  $\hat{\ell}$  is the orbital angular momentum for the collision, and  $\hat{V}(R)$  is the spin-independent electrostatic interaction potential. The Hamil-

tonian for the isolated alkali-metal atom may be written as

$$\hat{H}_M = A\hat{I} \cdot \hat{S} + 2\mu_0 B \hat{S}_z - B \frac{\mu_M}{I_M} \hat{I}_z, \quad (4)$$

where  $A$  is the hyperfine constant,  $\mu_0$  is the electron Bohr magneton,  $\mu_M$  is the nuclear magnetic moment of  $M$ , and the operators  $\hat{S}_z$  and  $\hat{I}_z$  yield the  $z$  components of the electron and nuclear spin of  $M$ . The interaction of the <sup>3</sup>He atom with a magnetic field is given by  $\hat{H}_{\text{He}} = -B(\mu_{\text{He}}/I_{\text{He}})\hat{I}_{z_{\text{He}}}$ . For the <sup>7</sup>Li and <sup>39</sup>K isotopes considered here,  $I_M=3/2$ . The spin-dependent term in Eq. (3) has the form [8]

$$\hat{H}_{\text{sd}} = A_F(R)\hat{I}_{\text{He}} \cdot \hat{S} + \gamma(R)\hat{\ell} \cdot \hat{S} + \Delta A(R)\hat{I} \cdot \hat{S}, \quad (5)$$

where the terms on the right-hand side describe the Fermi contact hyperfine interaction, the spin-rotation interaction, and the hyperfine frequency shift. In Eq. (5), we neglect the anisotropic part of the hyperfine interaction. This assumption is consistent with the procedure used to analyze experimental data [9,15]. The Fermi contact hyperfine constant is [10]

$$A_F(R) = \frac{16\pi\mu_0\mu_{\text{He}}}{3I_{\text{He}}} \rho(R). \quad (6)$$

In order to parametrize the spin-dependent Hamiltonian (5), we performed *ab initio* calculations of the Li-<sup>3</sup>He spin density using the coupled cluster method with single, double, and noniterative triple excitations [CCSD(T)] and unrestricted Hartree-Fock reference functions [16]. All calculations were performed using the ACES II package of programs [17]. The spin densities at the nuclei were computed with the  $\delta$ -function formalism from the CC relaxed density matrix. In order to ensure the correct behavior of the electronic wave function near the nuclei, we used a modified augmented correlation consistent polarized valence quintuple-zeta (aug-cc-pV5Z) basis for He obtained by fully decontracting the  $s$  functions and adding a sequence of three tight  $s$  functions with exponents forming a geometric progression. For Li, we adopted an aug-cc-pCVQZ (polarized core-valence quadruple-zeta) basis set with completely decontracted  $s$  functions augmented with four tight  $s$  functions. In both cases, the tight  $s$  functions were obtained by multiplying the largest  $s$  exponent of the parent basis set by a factor of 4. The calculated spin density at the Li nucleus is in close agreement with the value obtained from highly accurate calculations in Hylleraas coordinates [18].

Figure 1(a) compares the *ab initio* spin density of Li-<sup>3</sup>He with that computed using Herman's model [10] parametrized by  $\eta=9.5$  [19]. Although Eq. (1) overestimates the absolute magnitude of the spin density, its variation with  $R$  is reproduced surprisingly well. This is illustrated in Fig. 1(b), where we plot the refined estimate for the enhancement factor  $\eta$  obtained by substituting the *ab initio* spin density into Eq. (1). The *ab initio* enhancement factor varies slowly with  $R$ , and we find that  $\eta(R) \approx \eta(R_{\text{tp}})=2.5$ , where  $R_{\text{tp}}$  is the zero-energy turning point of the Li-<sup>3</sup>He interaction potential, denoted by the arrow in Fig. 1. In order to evaluate  $\eta$  for heavier alkali-metal atoms, we performed calculations of the frequency shift enhancement factor  $\kappa_0$  using Eq. (24) of

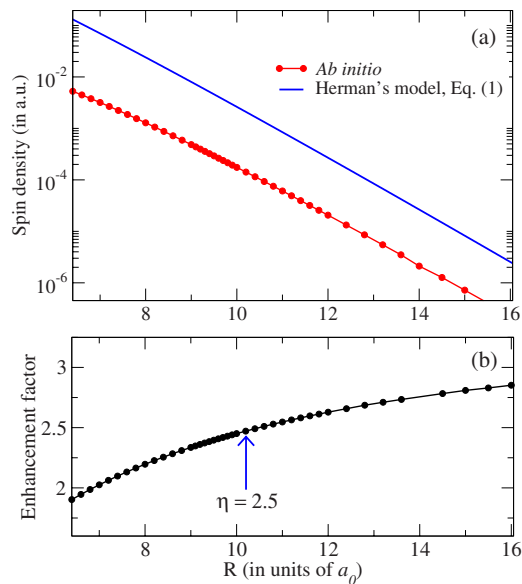


FIG. 1. (Color online) (a) The electron spin density for  $\text{Li-}^3\text{He}$ , Eq. (6), calculated as a function of the interatomic separation  $R$ : *ab initio* (circles) and Herman's model [10] (solid line). (b) The enhancement factor  $\eta$  calculated from Eq. (1) using the spin densities in the upper panel. The arrow marks the zero-energy turning point of the  $\text{Li-}^3\text{He}$  interaction potential [14].

Ref. [11] and accurate *ab initio* interaction potentials [14]. The electronic wave functions of the alkali-metal atoms were constructed from a numerical propagation of the Schrödinger equation, in which the interaction of the valence-core electrons was parametrically modeled [20]. The parameter  $\eta$  was varied until the calculated  $\kappa_0$  reproduced the measured values [13]. We obtain  $\eta=1.85$  for  $\text{K-}^3\text{He}$  and  $\eta=2.0$  for  $\text{Na-}^3\text{He}$ . These values are smaller than the lowest previous estimate of 5.8 [11]. We attribute the discrepancy to a different set of interaction potentials used to evaluate  $\kappa_0$  in this previous work.

In order to evaluate the rate constants for spin-changing transitions, we solve the multichannel scattering problem by expanding the total wave function of the collision complex in the basis  $|IM_I\rangle|SM_S\rangle|I_{\text{He}}M_{I_{\text{He}}}\rangle|\ell m_\ell\rangle$ , where  $|SM_S\rangle$  are the electron spin functions of the alkali-metal atom,  $|IM_I\rangle$  and  $|I_{\text{He}}M_{I_{\text{He}}}\rangle$  are the nuclear spin basis functions of  $M$  and  $^3\text{He}$ , and the functions  $|\ell m_\ell\rangle$  describe the orbital motion of the collision partners. Substitution of the expansion into the Schrödinger equation leads to a system of close-coupled equations, which is solved at fixed values of the collision energy and magnetic field.

Table I presents the calculated ratios of the rate constants for diffusion and spin exchange in collisions of Li and K atoms with  $^3\text{He}$ . The spin exchange occurs through the hyperfine transitions  $|F=2, m_F=2\rangle \rightarrow |F'=2, m'_F=1\rangle$  and  $|F=2, m_F=2\rangle \rightarrow |F'=1, m'_F=1\rangle$  accompanied by the nuclear spin-changing transition in  $^3\text{He}$   $|M_{I_{\text{He}}}=-1/2\rangle \rightarrow |M'_{I_{\text{He}}}=1/2\rangle$ . For both  $\text{Li-}^3\text{He}$  and  $\text{K-}^3\text{He}$ , the calculated ratios are much larger than the measured lower limits. The extremely slow spin exchange in  $M\text{-}^3\text{He}$  collisions reflects the exponential decay of the Fermi contact interaction with  $R$ . The repulsive interactions at short range prevent the collision partners from

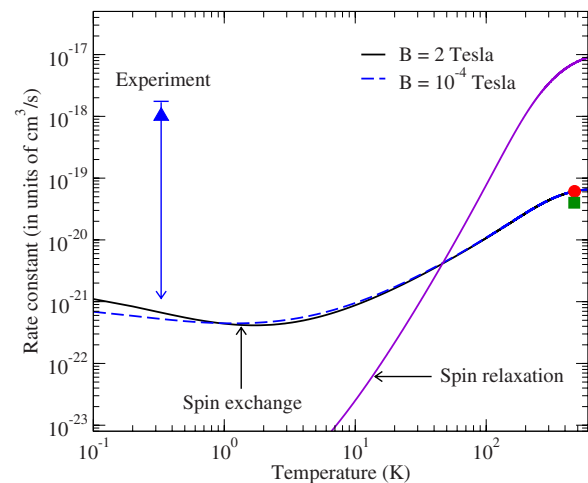


FIG. 2. (Color online) The calculated and measured spin exchange rates for  $\text{K-}^3\text{He}$  collisions as a function of temperature. The spin relaxation rate is also shown at a magnetic field of  $10^{-4}$  T. The upper limit to the spin exchange rate of magnetically trapped K measured in this work is shown by the triangle. The high-temperature rates measured in spin exchange optical pumping experiments are represented by the circle [9] and square [15].

reaching the region of strong Fermi contact interaction, causing suppression of spin exchange transitions.

Figure 2 shows the calculated temperature dependence of thermally averaged rate constants for spin exchange and spin relaxation in  $\text{K-}^3\text{He}$  collisions. The spin relaxation is mediated by the spin-rotation interaction [21], and it occurs through the same  $\Delta m_F = \pm 1$  transitions discussed above, but with no change in the nuclear spin state of  $^3\text{He}$ . The spin exchange rate exhibits a shallow minimum near 1 K, increases monotonically at larger temperatures, and shows little sensitivity to the magnetic field. The calculated spin exchange rate at  $T=320$  mK is  $5.3 \times 10^{-22}$   $\text{cm}^3/\text{s}$ , consistent with the experimentally derived upper limit of  $1.7 \times 10^{-18}$   $\text{cm}^3/\text{s}$ . Thus the spin depolarization of the alkali-metal atoms in  $^3\text{He}$  gas is much slower than in other magnetically trappable species, such as the noble-metal atoms [4] or  $^2\Sigma$  molecules [3]. At  $T=463.15$  K, our calculated spin exchange rate of  $6.1 \times 10^{-20}$   $\text{cm}^3/\text{s}$  is in excellent agreement with the experimental value of  $(6.1 \pm 0.4) \times 10^{-20}$  [9].

The temperature dependence of the spin relaxation rate shown in Fig. 2 is very steep, increasing by 6 orders of magnitude as the temperature is varied from 1 to 600 K (the spin exchange rates only gain a factor of  $\sim 10$ ). Such a dramatic effect is caused by the very fast exponential increase of the spin rotation constant  $\gamma(R)$  with decreasing  $R$  [8]. In addition, the matrix elements of the spin rotation interaction between the different spin states scale as  $[\ell(\ell+1)]^{1/2}$  [22]. At larger collision energies, higher partial waves contribute and the matrix elements increase considerably. We note that the Fermi contact interaction also increases exponentially with decreasing  $R$  (see Fig. 1). However, this dependence is less steep, so the variation of the spin exchange rates with  $T$  is not as dramatic.

The total spin depolarization rate at low collision energies is dominated by spin exchange. Since this channel is absent

for the  $^4\text{He}$  isotope, the results shown in Fig. 2 suggest that spin changing transitions in collisions with  $^4\text{He}$  will be further suppressed. This observation might explain why no spin relaxation of Li and Rb atoms was seen in a recent buffer-gas cooling experiment employing  $^4\text{He}$  [2]. Figure 2 demonstrates that transitions induced by the spin rotation interaction begin to take over as the collision energy increases and both spin exchange and spin relaxation mechanisms contribute equally for K- $^3\text{He}$  collisions at 45 K.

In summary, we have carried out a combined experimental and theoretical study of spin depolarization of the alkali-metal atoms in collisions with  $^3\text{He}$  atoms. Our *ab initio* calculations of the Li- $^3\text{He}$  electron spin density and the frequency shift enhancement factors have allowed us to extract the refined values of  $\eta=2.5$ , 2.0, and 1.85 for collision complexes of Li, Na, and K atoms with  $^3\text{He}$ . These values represent a significant improvement over the previous estimates of 5.8–12.6 [11,19]. Using the improved Fermi contact interaction parameters, we have calculated the probabilities for spin exchange and spin relaxation in  $M$ - $^3\text{He}$  collisions. The calculated spin exchange rate constants for Li- $^3\text{He}$  and K- $^3\text{He}$  are on the order of  $10^{-21}$  cm<sup>3</sup>/s, consistent with the

upper bounds derived from magnetic trapping experiments with Li and K atoms.

The results presented in Table I and Fig. 2 suggest that alkali-metal atoms confined in a magnetic trap have extremely long lifetimes (10–100 s) even in the presence of strong magnetic fields. This feature can be used to design high-precision atomic magnetometers based on cold alkali-metal vapor cells [2]. Another possible application is the use of buffer-gas-cooled Cs atoms to measure the electric dipole moment of the electron [23]. In addition, low decoherence rates of the alkali-metal atoms in a cold gas of  $^3\text{He}$  can be exploited in many interesting applications in quantum optics [7] and quantum information processing [24].

This work was supported by the Chemical Science, Geoscience, and Bioscience Division of the Office of Basic Energy Science, Office of Science, U.S. Department of Energy and NSF grants to the Harvard-MIT Center for Ultracold Atoms, Harvard University, and the Institute for Theoretical Atomic, Molecular, and Optical Physics at Harvard University and Smithsonian Astrophysical Observatory.

- 
- [1] I. K. Kominis, T. W. Kornack, J. C. Allred, and M. V. Romalis, *Nature (London)* **422**, 596 (2003).
  - [2] A. O. Sushkov and D. Budker, *Phys. Rev. A* **77**, 042707 (2008).
  - [3] J. D. Weinstein *et al.*, *Nature (London)* **395**, 148 (1998).
  - [4] N. Brahmns *et al.*, *Phys. Rev. Lett.* **101**, 103002 (2008).
  - [5] P. L. Anthony *et al.*, E-142 Collaboration, *Phys. Rev. Lett.* **71**, 959 (1993).
  - [6] M. S. Albert *et al.*, *Nature (London)* **370**, 199 (1994).
  - [7] T. Hong *et al.*, e-print arXiv:0805.1416.
  - [8] T. G. Walker and W. Happer, *Rev. Mod. Phys.* **69**, 629 (1997).
  - [9] E. Babcock *et al.*, *Phys. Rev. Lett.* **91**, 123003 (2003).
  - [10] R. M. Herman, *Phys. Rev.* **137**, A1062 (1965).
  - [11] D. K. Walter, W. Happer, and T. G. Walker, *Phys. Rev. A* **58**, 3642 (1998).
  - [12] M. V. Romalis and G. D. Cates, *Phys. Rev. A* **58**, 3004 (1998).
  - [13] E. Babcock, I. A. Nelson, S. Kadlecsek, and T. G. Walker, *Phys. Rev. A* **71**, 013414 (2005).
  - [14] H. Partridge, J. R. Stallcop, and E. Levin, *J. Chem. Phys.* **115**, 6471 (2001).
  - [15] G. Wang, Ph.D. thesis, California Institute of Technology, 2008.
  - [16] S. A. Perera, J. D. Watts, and R. J. Bartlett, *J. Chem. Phys.* **100**, 1425 (1994).
  - [17] J. F. Stanton *et al.*, computer program ACES II, Mainz-Austin-Budapest version, [www.aces2.de](http://www.aces2.de)
  - [18] Z.-C. Yan, D. K. McKenzie, and G. W. F. Drake, *Phys. Rev. A* **54**, 1322 (1996).
  - [19] T. G. Walker, *Phys. Rev. A* **40**, 4959 (1989).
  - [20] M. Marinescu, H. R. Sadeghpour, and A. Dalgarno, *Phys. Rev. A* **49**, 982 (1994).
  - [21] T. G. Walker, J. H. Thywissen, and W. Happer, *Phys. Rev. A* **56**, 2090 (1997).
  - [22] R. V. Krems and A. Dalgarno, *J. Chem. Phys.* **120**, 2296 (2004).
  - [23] M. Bijlsma, B. J. Verhaar, and D. J. Heinzen, *Phys. Rev. A* **49**, R4285 (1994).
  - [24] C. W. Chou *et al.*, *Nature (London)* **438**, 828 (2005).